A Short-term Wind Speed Prediction Method Based on the DGA-BP Neural Network

Lingzhi Wang*, Cheng Li, Chenyang Li

***Abstract*—Wind energy is pollution-free and renewable, and the stable operation of wind farms depends significantly on the accuracy of wind speed predictions. The BP neural network has the advantage of error reverse transmission and is commonly used in wind speed prediction. However, its parameter selection is sensitive and prone to fall into the local optimum. Therefore, this study introduces a dual-layer genetic algorithm (DGA) to optimize the BP neural network's initial weights and thresholds. By separating the genetic algorithm (GA) into global and local optimization, a DGA-BP wind speed prediction model is constructed. With the purpose of verifying the wind speed prediction effect of the DGA-BP model, comparative experiments of the five models (BP, GA-BP, SSA-BP, SAO-BP, and DGA-BP) were implemented for wind prediction and prediction errors by using three datasets. The results indicate that the DGA-BP model has a better accuracy over the other four models in wind speed prediction and has obvious advantages. In addition, the mean absolute error (MAE), mean square error (MSE), root mean square error (RMSE), and mean absolute percentage error (MAPE) calculated values of the DGA-BP model are smaller than the other four models regardless of dataset 1, dataset 2 or dataset 3, which further demonstrating the viability and superiority of the DGA-BP neural network in predicting wind speed.**

***Index Terms*—Dual-layer genetic algorithm, Wind speed prediction, Neural networks, Prediction accuracy**

I. Introduction

WIND energy, a significant component of the new energy industry, consistently pushes the world's energy transition and advancements in sustainable development [1]. By 2022, China had installed roughly 370 million kilowatts of wind power capacity, which has grown compared with 2021. At the same time, China's wind power generation reached 1.19 trillion kilowatt hours, an increase of 21% over the previous year's power generation. In the future, wind power will maintain a stable growth trend.

As one of the emerging industries in China, the wind power industry has developed fast and plays a vital role in the power system [2, 3]. However, wind speed is the most significant factor affecting wind power generation [4], and wind speed instability poses certain challenges to grid power quality. Larger or smaller wind speeds will cause fluctuations in wind turbine output, further impacting the power quality of the grid and the steady operation of the power system [5]. Accurately forecasting wind speed helps mitigate the effects of output power fluctuations on the power grid and improves wind farm efficiency [6]. Moreover, the stability and dependability of the power grid will push the wind energy sector's sustainable growth. Thus, forecasting wind speed will become increasingly crucial for wind energy farms [7].

Wind speed prediction methods can be divided according to the models: statistical methods, physical models, and machine learning [8]. For statistical methods, historical wind speed data are used for statistical analysis with common models including the ARIMA model and the GARCH model. As for the physical model, the physical characteristics and dynamic principles of the wind field are employed to simulate the variation in wind speed and produce modeling forecasts. The machine learning method requires vast historical data to be separated into training and test sets, and uses the trained models to predict data. The common machine learning models include the artificial neural network [9], the decision tree [10], and the support vector machine [11].

Neural networks are a prevalent technique in predicting wind speed due to their high flexibility and suitability for nonlinear problems. They can handle large volumes of data and enhance prediction accuracy. When dealing with the practical problems of large-scale data, BP neural networks are widely regarded as one of the most commonly used solutions in the field of neural networks [12-14]. Its major objective is continuously improving the network's efficiency and precision by modifying its weights and thresholds through forward transmission of data and reverse transmission of errors [15]. After multiple iterative trainings, a well-trained network model is finally obtained, which can be utilized to forecast and classify new sample data.

Consequently, BP neural networks effectively resolve large-scale data problems and achieve accurate predictions through continuous optimization and learning processes. However, parameter selection significantly influences BP neural networks, and even minor parameter adjustments directly impact the model's performance [16]. Furthermore, the network is susceptible to being trapped in local optimal solutions and fails to reach the desired global solution. These shortcomings can be overcome with appropriate approaches.

As a result, numerous optimization algorithms have been proposed for optimizing BP neural networks. Liu *et al.* [17] optimized the Elman network using an improved particle swarm optimization algorithm, constructed a wind speed prediction model, and verified it through simulation

Manuscript received September 27, 2023; revised February 27, 2024.

This work was supported in part by the National Natural Science Foundation of China (52177194, 62073259).

Lingzhi Wang is a professor at Xi'an University of Posts and Telecommunications, Xi'an 710121, China (corresponding author to provide email: wlzmary@126.com).

Cheng Li is a postgraduate student of the School of Automation, Xi'an University of Posts and Telecommunications, Xi'an 710121, China (email: 2056866020@qq.com).

Chenyang Li is a postgraduate student of the School of Automation, Xi'an University of Posts and Telecommunications, Xi'an 710121, China (email: xupt_lcy@163.com).

experiments. Fang *et al.* [18] conducted experiments using historical wind speed data from a wind farm and developed a genetic algorithm-based optimization for the BP neural network. This resulted in the creation of a GA-BP prediction model that exhibited excellent performance. Long *et al.* [19] used convolutional neural networks to extract features from the denoised wind speed sequence, and then optimized the long short-term memory network using the sparrow search algorithm to construct a wind speed prediction model. Shi *et al.* [20] proposed a ConvLSTM-ConvGRU hybrid wind speed prediction model using the wind speed dataset provided by the National Center for Environmental Forecasting (NCEP). This method proved its ability to accurately forecast wind speed in Yunnan's wind farms. The application of these optimization algorithms effectively assists neural networks in achieving better results in their search for global optimal solutions, thereby improving the accuracy of prediction results. Therefore, optimization algorithms enhance overall performance and the prediction capacity of neural networks.

In this study, a dual-layer genetic algorithm (DGA) is proposed to tune the parameters of the BP neural network for predicting wind speed. Three test functions were first used to evaluate the convergence process of the GA, SSA (Sparrow Search algorithm), SAO (Snow Ablation Optimizer), and DGA algorithms. Then, the DGA-BP model is established and served to predict wind speed. Utilizing wind speed data from an American wind farm in Ohio, the DGA-BP model's performance in wind speed prediction was verified through comparative simulation experiments with the BP, GA-BP, SSA-BP and SAO-BP models, and was further assessed by comparing the four error indicators of the five models.

II. DGA-BP Neural Network

A. Neural Networks

BP neural networks are primarily employed to address tasks such as function approximation, classification, pattern recognition, and regression. Their adaptability enables them to handle various nonlinear interactions and high-dimensional data. In practical applications, BP neural networks are frequently used to handle these problems and accomplish precise prediction, classification, and identification tasks [21]. Whether it involves numerical calculations, image recognition, or data analysis, BP neural networks prove to be effective tools. The BP neural network, which is seen in Fig. 1, has three or more layers, and each comprises numerous neurons [22]. The neurons in the left and right layers of the network are fully connected, whereas the upper and lower layers are not.

In Fig. 1, z_1, z_2, …, z_n represents the input of the BP neural network, y_1, y_2, …, y_n represents the output, ω_{ij} is the connection weight between the input layer and the hidden layer, and ω_{jk} is the connection weight between the hidden layer and the output layer.

By continually sending data from the training set from the input layer through the hidden layer to the output layer, the BP neural network uses the training set to train a good training model. Then, the trained model has a predictive function. However, there are some drawbacks to the network. A lot of data, for instance, will slow the algorithm's learning pace, and sink into the local optimal solution when configuring the network parameters, thus, further lowering the network's predictive performance. Therefore, this research introduces a genetic algorithm-based optimization strategy to enhance the BP neural network and increase its prediction accuracy.

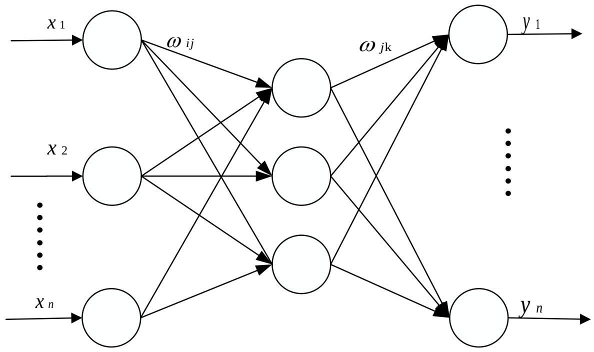

Fig. 1. Neural network structure

B. GA-BP Neural Network

This research offers an improved technique incorporating genetic algorithm to optimize the initial network parameters to address the faults and limits of the BP neural network. By utilizing genetic algorithm, the initial parameters of the network can be searched and optimized for better performance. By simulating the process of biological evolution, genetic algorithm continuously iteratively adjusts and select the parameters of the network, thus the network can more easily adjust to the task's demands [23].

The GA-BP neural network's nucleus is: through the selection, crossing, mutation, and other operations of species in nature, the population continues to evolve [24]. At the same time, the BP neural network is adjusted to obtain the optimal weights and thresholds for the network [25]. Its objectives are to improve network learning efficiency and hasten network convergence. The GA-BP flowchart is shown in Fig. 2.

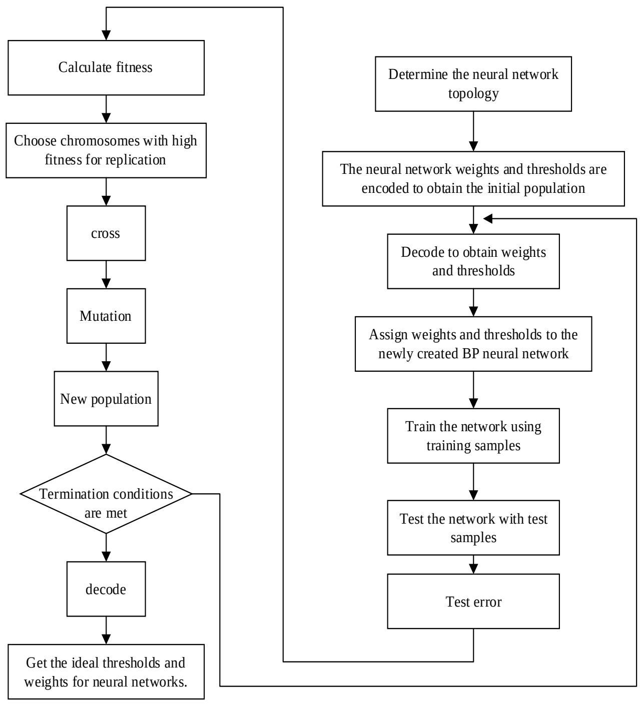

Fig. 2. Flow chart of the GA-BP neural network

Genetic algorithm is utilized to determine the best network parameters so that the network is more stable and can successfully avoid the drawbacks of the BP neural network [26].GA-BP is mostly exploited to process large-scale, high-dimensional datasets, and has succeeded in forecasting, logistics management, and image recognition.

C. DGA-BP neural network

In the above GA-BP, the genetic algorithm enables the BP network to find the optimal solution, but due to its randomness, it is hard to ensure that the global optimal solution will always be attained. Besides, although GA-BP has improved over the shortcomings of BP in overfitting, this problem still exists. Therefore, based on the GA-BP, this paper further improves the genetic algorithm given its shortcomings, and proposes a dual-layer genetic algorithm to optimize the wind speed prediction model of the BP neural network.

The algorithm adopts a dual-layer optimization strategy, which has more advantages than the traditional genetic algorithm. The dual-layer genetic algorithm executes global and local searches to achieve rapid convergence to the global optimal solution and unleash the full potential of the genetic algorithm. Moreover, the algorithm has higher search accuracy, and avoids the local optimization problem of traditional genetic algorithm.

The outer layer is the global search layer, which performs a global search of the main population by applying the genetic algorithm. This layer includes operations such as population initialization, crossover, and mutation, and is designed to find, evaluate, and select potential solutions in a broad solution space, often referred to as subproblems. The outer layer's function is to search the entire search space for the best solution.

The inner layer is the local search layer used to further refine the solution obtained by the global search. The solution obtained by the outer layer (called subpopulation) is again optimized using a genetic algorithm. Each subpopulation undergoes a relatively independent evolutionary process, indicating that each subpopulation seeks a better solution locally through crossover, mutation, selection, and other operations. In this way, each subpopulation can focus on exploring a specific search space, improving the quality of population and global search efficiency. The evolutionary process of subpopulations can be thought as a local search for specific subpopulations, and when the algorithm converges, the optimal individual will be used as a new population of the outer genetic algorithm. The outer population can then use the better solution found by the inner genetic algorithm to conduct a global search and further improve the performance of the outer population. The purpose of the inner layer is to perform fine optimization near the solution obtained by the global search to obtain a better solution.

Fig. 3 is the dual-layer genetic algorithm's BP neural network flowchart. The algorithm's steps are as follows:

Step 1: Neural network initialization. Calculate the number of the nodes in input, output, and hidden layers based on the features of the data. Through coding function of the genetic algorithm, the initial network characteristics including the starting population size are encoded.

Step 2: Decode [27]. The weights and thresholds are assigned to the DGA-BP neural network for network training in the global search layer.

Step 3: Calculate the hidden layer's output. Equation (1) calculates the output Hid_j based on the input variable z_i, weight ω_{ij}, and threshold a_j. Equation (2) is the excitation function chosen in this paper.

$$Hid_j = f(\sum_{i=1}^{n}\omega_{ij}z_i - a_j),\ j = 1,2,...,l \tag{1}$$

$$f(z) = 1/(1+e^{-z}) \tag{2}$$

Step 4: Calculate the output of the output layer. Out_k is calculated using Equation (3) in accordance with the hidden layer's output Hid_j, weight ω_{jk}, and threshold b_k.

$$Out_k = \sum_{k=1}^{l} Hid_j\omega_{jk} - b_k,\ k = 1,2,..,m \tag{3}$$

Step 5: Calculate the network prediction error. The prediction error is the deviation between the expected output and the predicted output, and its calculation formula is shown in (4).

$$err_k = Act_k - Out_k,\ k = 1,2,...,m \tag{4}$$

Step 6: Calculate the new network weights. According to the prediction error err_k and the learning rate η, the weights ω_{ij} and ω_{jk} are calculated by Equations (5) and (6).

$$\begin{gathered}\omega_{ij} = \omega_{ij} + \eta Hid_j(1-Hid_j)\sum_{k=1}^{m}\omega_{jk}\cdot err_k \\ i = 1,2,...,n;\ j = 1,2,...,l\end{gathered} \tag{5}$$

$$\begin{gathered}\omega_{jk} = \omega_{jk} + \eta Hid_j\cdot err_k \\ j = 1,2,...,l;\ k = 1,2,...,m\end{gathered} \tag{6}$$

Step 7: Calculate the new network thresholds. According to the prediction error err_k and the learning rate η, the thresholds a_j and b_k are calculated by Equations (7) and (8).

$$\begin{gathered}a_j = a_j + \eta Hid_j(1-Hid_j)\sum_{k=1}^{m}\omega_{jk}\cdot err_k \\ j = 1,2,...,l\end{gathered} \tag{7}$$

$$b_k = b_k + err_k,\ k = 1,2,...,m \tag{8}$$

Step 8: Utilizing the training data, continuously pass the error value backward to update the network parameters until obtaining the best trained model. Substitute the updated weights and thresholds into the DGA-BP neural network.

Step 9: Calculate and compare the fitness value of each individual, and select chromosomes with high fitness values as the optimal individual. A new population can be obtained by performing operations such as copying, crossing, and mutating. Doing so can promote the evolution and optimization of the population. The evaluation index of the fitness function chosen in this paper is the average mean square error.

Step 10: Check to see if the algorithm converges in accordance with the end conditions that have been established (the maximum iterations and the smallest goal error). If the neural network has converged, assign the results obtained by the global search to the local search layer for a more accurate search; Otherwise, return to **Step 2** to proceed to the next iteration.

Step 11: After calculating and assessing the fitness value of the subpopulation's members, perform crossover, selection, mutation and other operations, and start the population iteration of the local search layer.

Step 12: Determine whether the local genetic algorithm converges according to the preset end conditions (the maximum iterations and the smallest goal error). If convergence, the decoding operation is performed, and the result with the best network weights and thresholds is output; Otherwise, return to **step 2** to proceed to the next iteration.

Step 13: Use the global optimal values produced by the dual-layer genetic algorithm as the optimal weights and thresholds of the BP neural network, and then make data predictions.

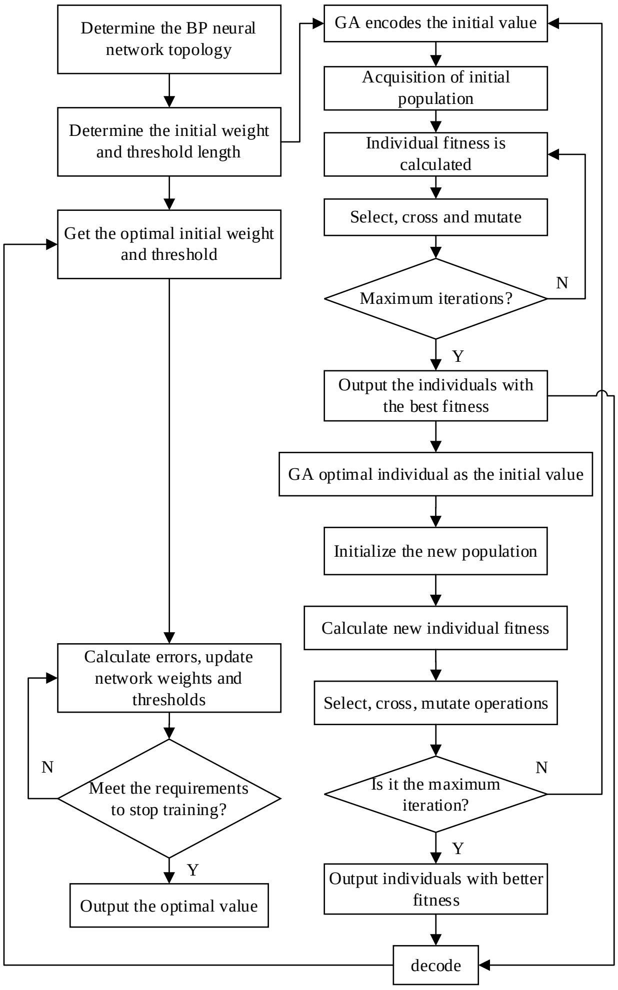

Fig. 3. Flow chart of the DGA-BP neural network

By combining global and local optimizations, the dual-layer genetic algorithm can search broadly throughout the population and conduct indepth searches near the local area. This would increase the efficiency and accuracy of the optimization algorithm, resulting in better results. The dual-layer genetic algorithm effectively addresses complicated problems, particularly those with a large search space, multimodal functions, or nonlinear problems. Therefore, the corresponding DGA-BP neural network can achieve superior performance.

D. Algorithm performance testing

To assess the performance of the proposed DGA algorithm, three test functions are shown in Table I.

In Table I, F_1 is a unimodal function, F_2 is a multimodal function, and F_3 is a multimodal function with a fixed dimension of 2. Each algorithm is initialized with a population size of 30, a maximum of 1000 iterations, and a dimension of 30. Fig. 4 illustrates the convergence process of the four algorithms (GA, SSA, SAO, and DGA) across three test functions.

TABLE I
TEST FUNCTIONS

Function	Boundary	Optimal solution
$F_1(x)=\sum_{i=1}^{n-1}\left[100\left(x_{i+1}-x_i^2\right)^2+\left(x_i-1\right)^2\right]$	$[-30,30]$	0
$F_2(x)=\frac{1}{4000}\sum_{i=1}^{n}x_i^2-\prod_{i=1}^{n}\cos\left(\frac{x_i}{\sqrt{i}}\right)+1$	$[-600,600]$	0
$F_3(x)=\left(\frac{1}{500}+\sum_{i=1}^{25}\frac{1}{j+\sum_{i=1}^{2}\left(x_i-aij\right)^6}\right)^{-1}$	$[-65,65]$	0.998

As shown in Fig. 4, the DGA algorithm has always a smaller fitness value in fewer iterations than the other three algorithms for three test functions. This suggests that the DGA algorithm has higher convergence accuracy and faster convergence speed.

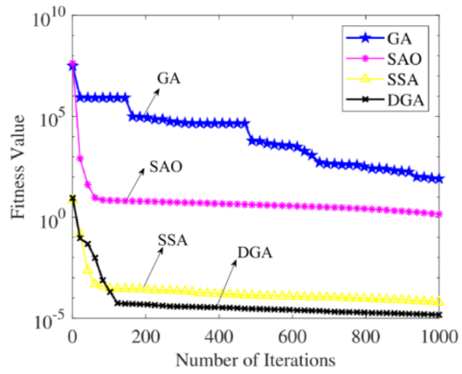

(a) F_1

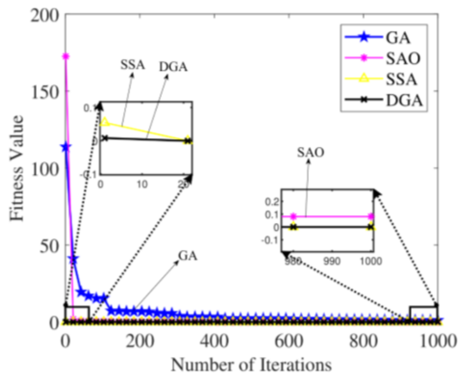

(b) F_2

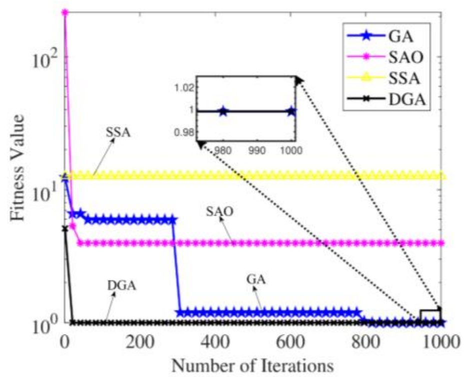

(c) F_3

Fig. 4. Convergence curve of the test function

III. Application of The DGA-BP Neural Network in Wind Speed Prediction

D. Data Preprocessing

Wind speed data were collected by the data acquisition and monitoring control system, and the experimental data of wind turbines form a wind farm in Ohio, USA, were chosen from the historical operation data. To test the viability and effectiveness of the DGA-BP prediction model, the wind speed data collected by three different numbered wind turbines in the wind farm from 0:00 on August 1 to 19:00 on August 18 in 2017 (data from the wind turbine A-02 are marked as dataset 1, data from the wind turbine A-09 are dataset 2, and data from the wind turbine A-13 are dataset 3) was used for simulation experiments. The data interval for each dataset is 5 minutes, and the effective information is protected by data desensitization. Normalization is performed using the maximum-minimum method [28], as shown in Equation (9).

$$Z_k = (Z_k - Z_{\min}) / (Z_{\max} - Z_{\min}) \qquad (9)$$

This study uses the rolling forecasting method. That is, predict Z_{n+1} with the data Z_1, Z_2, …, Z_n, the data Z_2, Z_3, …, Z_{n+1} for predicting Z_{n+2}. Here, we take n=9. After screening, the datasets collected by different numbered wind turbines were selected for verification, and each dataset has 4110 sets of data. Among them, 4000 sets of data from each dataset were utilized as training samples for the BP neural network, whereas the remaining 110 sets of data are utilized as testing samples to prove the DGA-BP neural network's accuracy in predicting wind speed.

E. Error evaluation indicators

To more precisely evaluate the efficacy of the DGA-BP neural network prediction model, mean absolute error (MAE), mean square error (MSE), root mean square error (RMSE), and mean absolute percentage error (MAPE) are introduced as error measures, and Equations (10)-(13) show the computation formulas.

$$\text{MAE} = \frac{1}{M}\sum_{i=1}^{M} |z(i) - \tilde{z}(i)| \qquad (10)$$

$$\text{MSE} = \frac{1}{M}\sum_{i=1}^{M} (z(i) - \tilde{z}(i))^2 \qquad (11)$$

$$\text{RMSE} = \sqrt{\frac{1}{M}\sum_{i=1}^{M} (z(i) - \tilde{z}(i))^2} \qquad (12)$$

$$\text{MAPE} = \left|z(i) - \tilde{z}(i)\right| / \left|z(i)\right| \qquad (13)$$

M is the number of samples, whereas $z(i)$ and $\tilde{z}(i)$ are the measured wind speed data and the anticipated wind speed data based on five models.

F. Establishment of the DGA-BP model

In the genetic algorithm, each individual is evaluated using a fitness function, and during evolution, its odds of survival and reproduction are calculated based on their fitness values. MSE is chosen as the fitness function to calculate the fitness value of each individual, the lower the fitness value, the better the individual. This demonstrates that the algorithm's weights and thresholds are improved, which will increase the accuracy and bring the neural network's prediction outputs closer to the actual measured values.

With the aid of empirical formulas and the examination of experimental data, when *inputnum*=9 and *outputnum*=1, the number of the nodes in hidden layer is accurately calculated. The empirical formula is shown in Equation (14).

$$hiddennum = \sqrt{inputnum + outputnum} + a \qquad (14)$$

where *hiddennum*, *inputnum*, and *outputnum* indicate the number of the nodes in hidden, input, and output layers, respectively. The number of the nodes in hidden layer is changed by the constant a, which has a range of 1 to 10 [29].

After conducting numerous trials, trainlm is chosen as the training function. When the BP neural network achieves the best prediction effect, the number of the nodes in hidden layer is determined as 8 for dataset 1, 11 for dataset 2 and 6 for dataset 3. Take the learning rate as 0.01, the minimum target error as 10^{-5}, and the number of training repetitions as 10^3 times. The initial population size is 50 for the outer genetic algorithm of the DGA-BP neural network, and the maximum evolutionary algebra is 100. The cross operation uses a two-point crossover, the selection operation uses the roulette approach, and the cross probability is 0.8. The mutation operation uses Gaussian mutation, and the probability is 0.2. In addition, for the DGA-BP neural network's internal genetic algorithm, the inner layer often sets a smaller and more accurate population size than the setting of the outer genetic algorithm. In our simulation, the initial population size is 30, and the maximum evolutionary algebra is 50.

Figs. 5(a), 6(a), and 7(a) represent the change in the fitness values of the outer genetic algorithm for three datasets. The optimal fitness values of the outer layer are 0.322037, 0.324113 and 0.364087, and the average fitness values were 0.325428, 0.334366 and 0.38251, respectively.

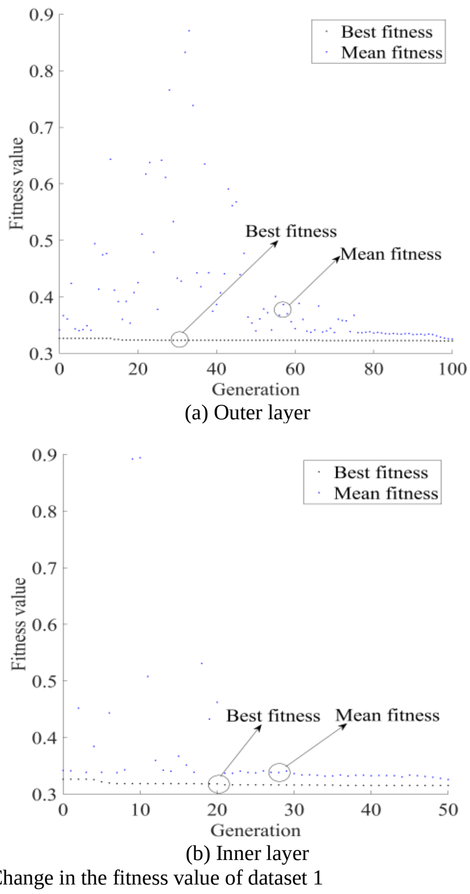

Fig. 5. Change in the fitness value of dataset 1

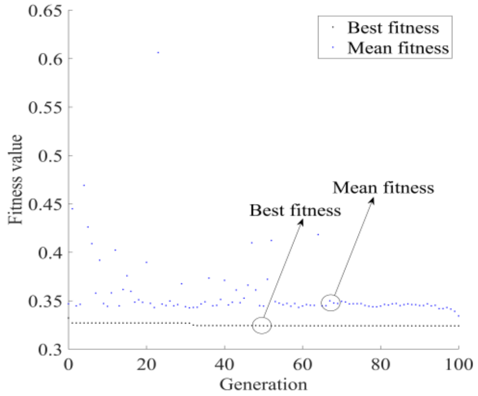

(a) Outer layer

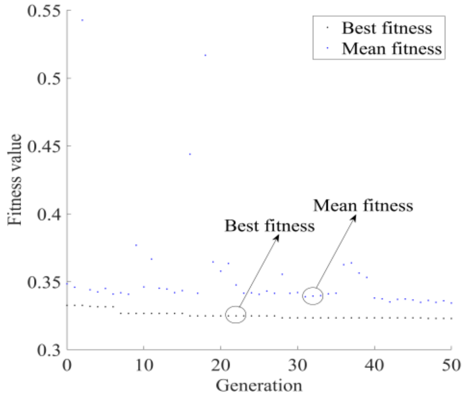

(b) Inner layer

Fig. 6. Change in the fitness value of dataset 2

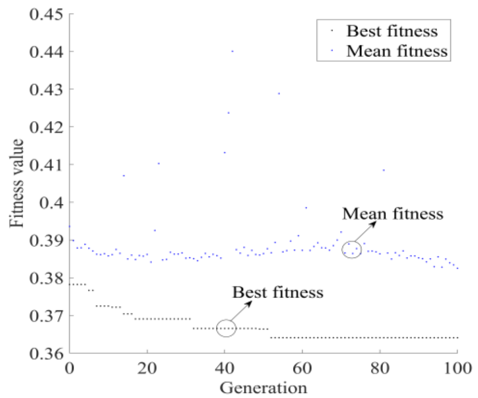

(a) Outer layer

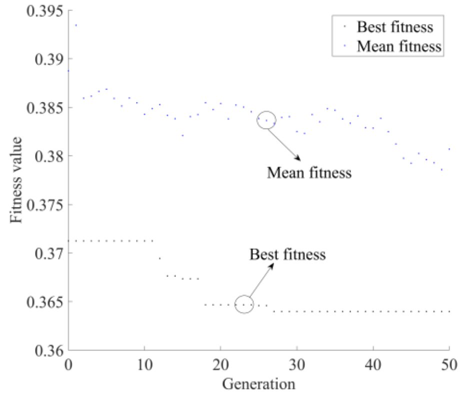

(b) Inner layer

Fig. 7. Change in the fitness value of dataset 3

Figs. 5(b), 6(b), and 7(b) represent the change in the fitness values of the inner genetic algorithm for three datasets. The optimal fitness values of the inner layer are 0.315384, 0.322934 and 0.363982, and the average fitness values were 0.325803, 0.334333 and 0.380701, respectively.

From Figs. 5-7, it is clear that the optimal fitness values of the inner layer of the three datasets are lower than those of the outer layers. Declining of three fitness values indicate that the fitness values become smaller when the optimal value of the global optimization of the outer genetic algorithm is used as the initial value of the local optimization of the inner genetic algorithm. The individual is better when the fitness value is lower, which improves the network's weights and thresholds as well as the prediction effect of the model.

D. Experimental results and analysis

Figs. 8, 9, and 10 show the experimental results of three datasets under five prediction models (BP, GA-BP, SSA-BP, SAO-BP, and DGA-BP), respectively. (a) represents the prediction result graph and (b) is the error comparison chart.

From the experimental results in Figs. 8-10, it can be seen that the prediction results of the DGA-BP model are closer to the true values. The error curve of most data points predicted by the DGA-BP model is closer to 0.

To further assess the effectiveness of the BP, GA-BP, SSA-BP, SAO-BP, and DGA-BP models in wind speed prediction, error indicators of the five models for the three datasets are calculated respectively as demonstrated in Table II. Moreover, in order to observe the performance of each model more intuitively, a histogram is utilized to display the error evaluation indexes of each model for the three datasets, as shown in Fig. 11.

TABLE II
Error indicators of five prediction models (BP, GA-BP, SSA-BP, SAO-BP, and DGA-BP) based on different datasets

	Prediction models	Error Indicators			
		MAE(m/s)	MSE(m/s)	RMSE(m/s)	MAPE
Dataset 1	BP	0.3594	0.2004	0.4477	6.573%
	GA-BP	0.3454	0.1870	0.4324	6.419%
	SSA-BP	0.3484	0.1913	0.4374	6.522%
	SAO-BP	0.3406	0.1870	0.4324	6.286%
	DGA-BP	0.3338	0.1735	0.4166	6.222%
Dataset 2	BP	0.3629	0.2170	0.4658	6.533%
	GA-BP	0.3624	0.2079	0.4560	6.503%
	SSA-BP	0.3516	0.2046	0.4523	6.233%
	SAO-BP	0.3511	0.2082	0.4563	6.277%
	DGA-BP	0.3417	0.1987	0.4458	6.131%
Dataset 3	BP	0.4239	0.2666	0.5163	8.007%
	GA-BP	0.4103	0.2547	0.5046	7.705%
	SSA-BP	0.4188	0.2560	0.5060	7.894%
	SAO-BP	0.4109	0.2601	0.5100	7.817%
	DGA-BP	0.4062	0.2476	0.4976	7.633%

From the error calculations of five prediction models in Table II, the four errors of the DGA-BP model are decreased to varied degrees in comparison to those of the BP, GA-BP, SSA-BP, and SAO-BP models. Among them, compared with the unoptimized BP network, MAE, MSE, RMSE, and MAPE calculated from the optimized network based on double-layer genetic algorithm decreased by 7.1%, 13.4%, 6.9%, and 5.3% respectively in dataset 1, descended by 5.8%, 8.4%, 4.3%, and 6.2% respectively in dataset 2, and declined by 4.2%, 7.1%, 3.6%, and 4.7% respectively in dataset 3. As can be clearly seen from Fig. 11, the DGA-BP prediction model has significantly smaller error indexes and outstanding optimization performance than the other four models. Therefore, compared to the BP, GA-BP, SSA-BP, and SAO-BP prediction models, the DGA-BP wind speed prediction model developed in this research has fewer errors and higher prediction accuracy, and the forecast values are closer to the actual values, with better prediction performance.

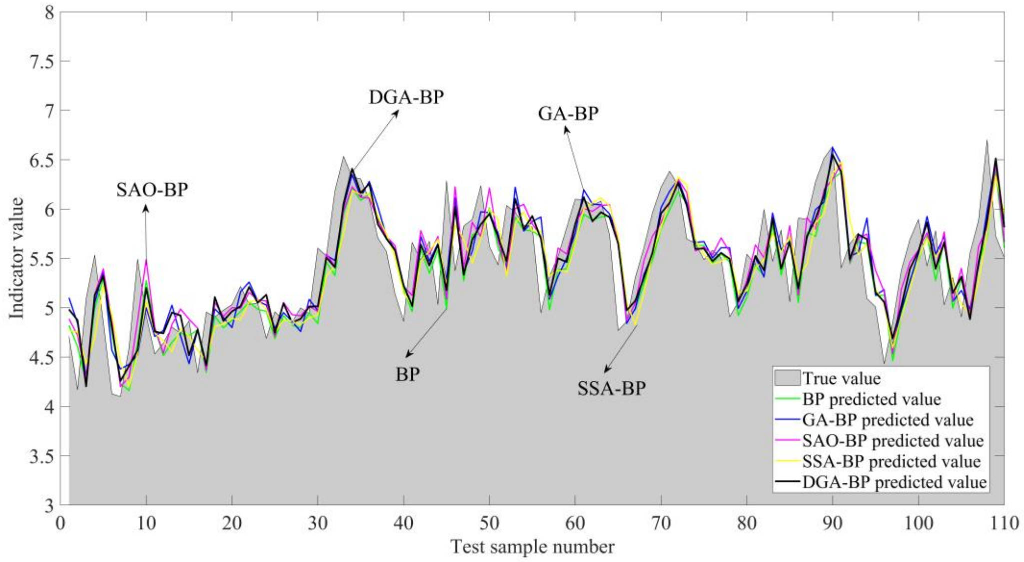

(a) Wind speed predicted results

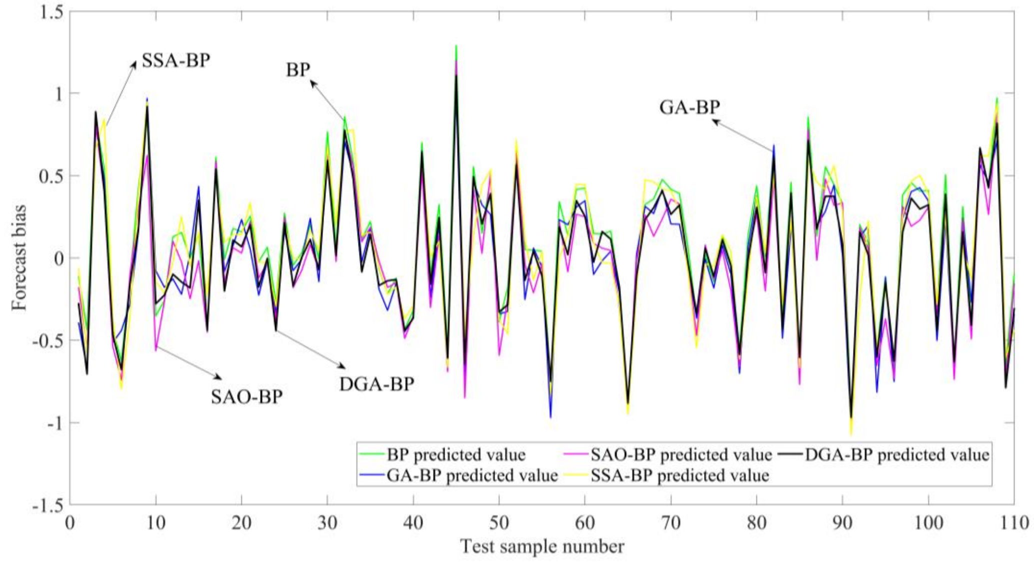

(b) Errors of the five models

Fig. 8. Experimental results for dataset 1

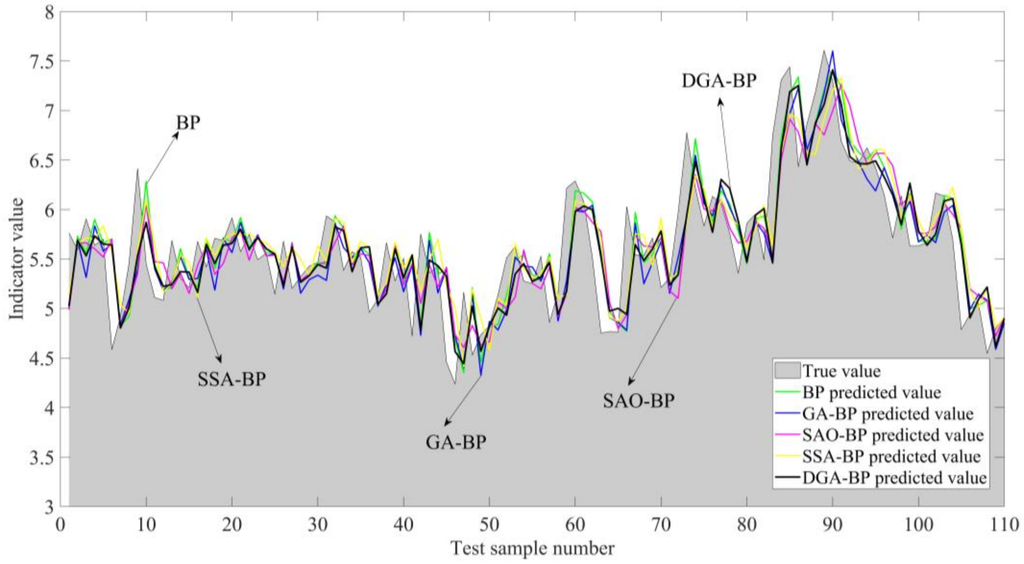

(a) Wind speed predicted results

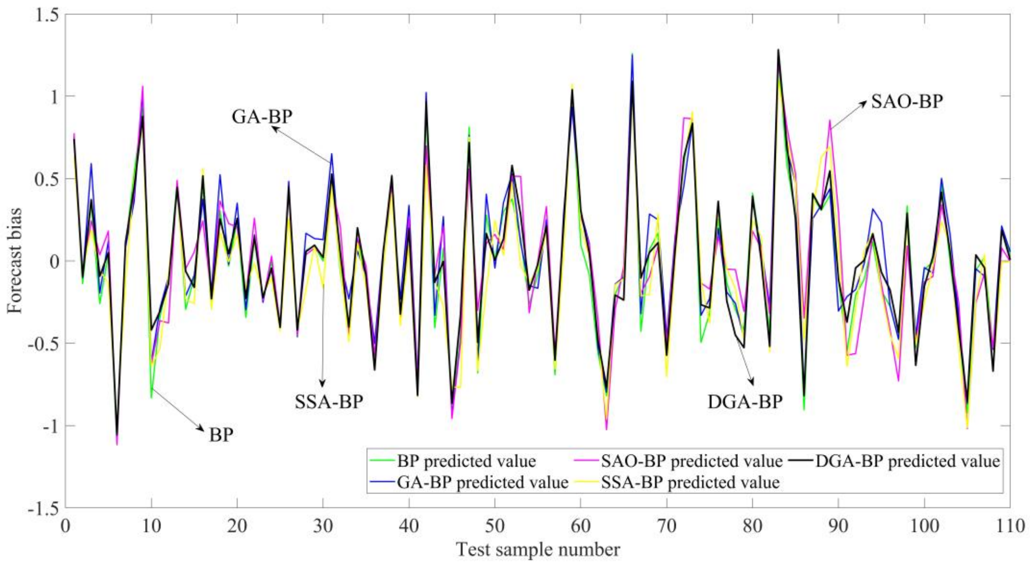

(b) Errors of the five models

Fig. 9. Experimental results for dataset 2

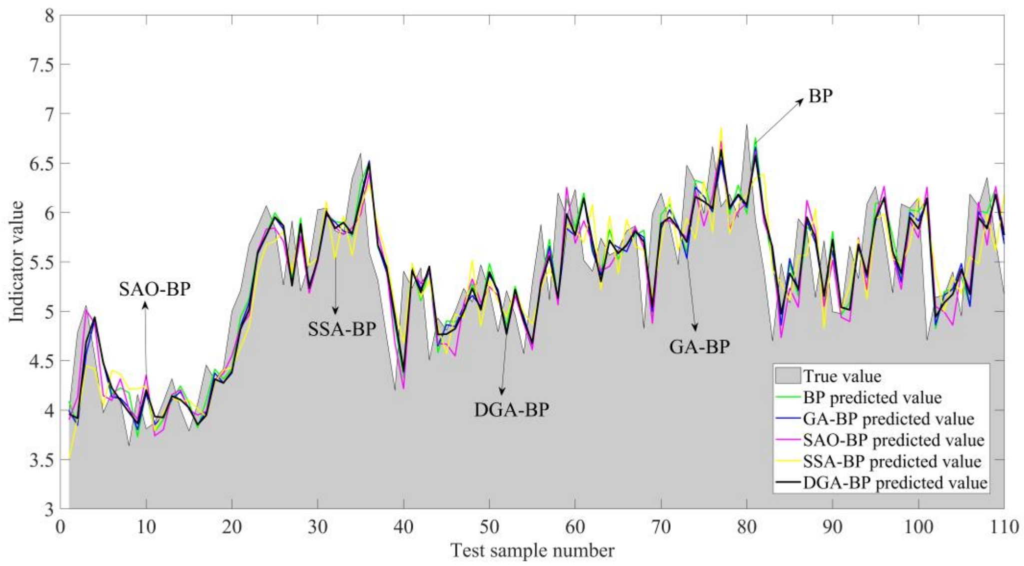

(a) Wind speed predicted results

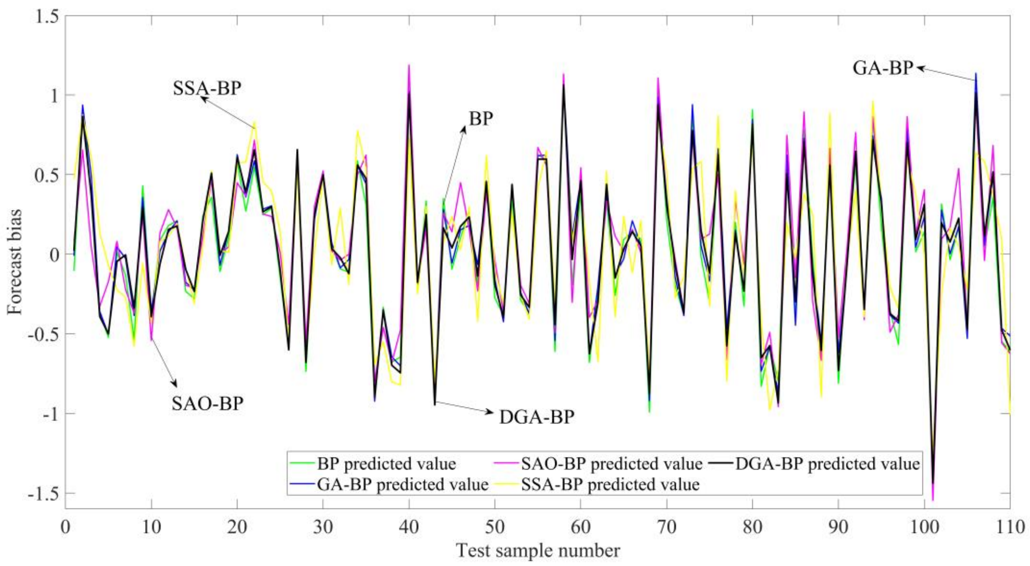

(b) Errors of the five models

Fig. 10. Experimental results for dataset 3

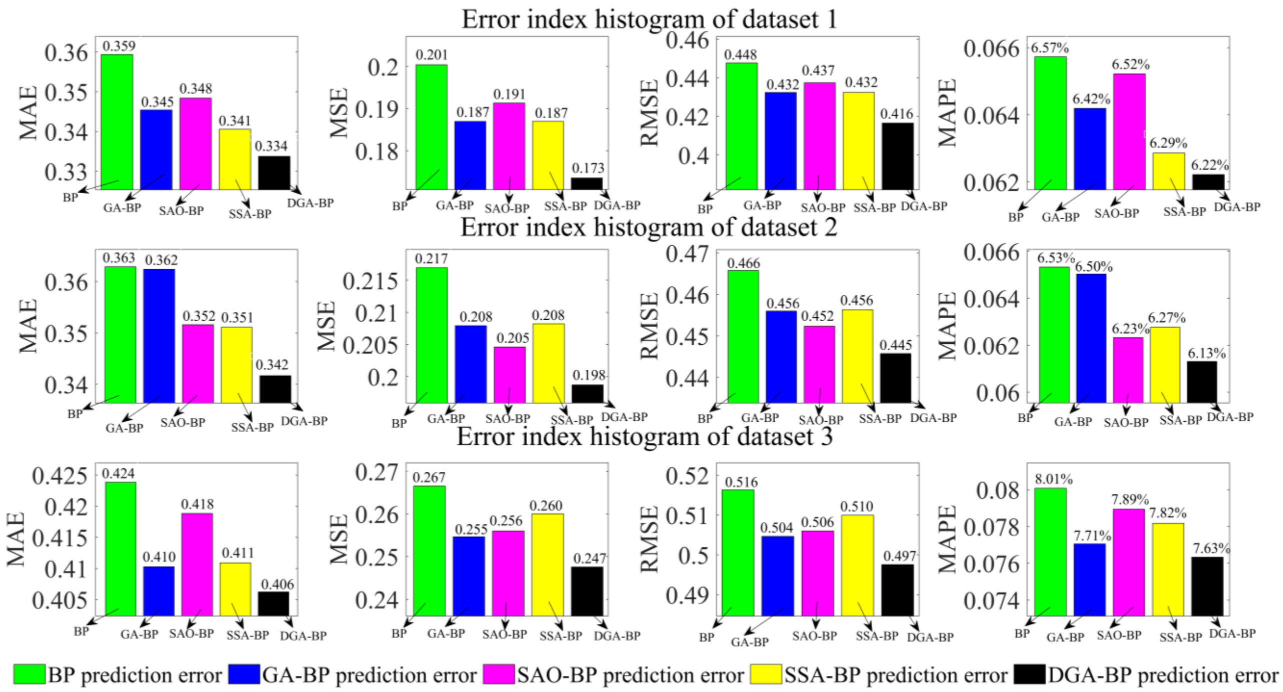

Fig. 11. Error index histogram of three datasets

IV. Conclusion

In this study, an enhanced genetic algorithm-based BP neural network prediction model is established for wind speed. The model uses a dual-layer genetic algorithm for global optimization and local optimization, taking the global optimization solution as the initial value for local optimization in the second phase, ultimately deriving the optimal parameters of the BP neural network. Through simulation experiments, the wind speed prediction curves and error curves of five prediction models for three datasets indicate that the DGA-BP model exhibits a better prediction effect than the BP, GA-BP, SSA-BP, and SAO-BP models. The error curve of the DGA-BP model approaches zero more closely at most data points than the other four models.

Additionally, the calculations of average absolute error, mean square error, root mean square error, and mean absolute percentage error of the five models revealing that the DGA-BP model yields the lowest error. These outcomes further validate the accuracy and suitability of the prediction model for forecasting future wind speeds. In conclusion, accurate wind speed predictions enable wind farms to optimize energy output, proactively anticipate changes in wind energy resources, and adjust power generation equipment operations to enhance wind energy utilization efficiency and economic viability.

References

[1] H. Chen, J. Z. Zhang, Y. B. Tao, and F. L. Tan, “Asymmetric GARCH type models for asymmetric volatility characteristics analysis and wind power forecasting”, *Protection and Control of Modern Power Systems*, vol. 4, no. 2, pp. 1547-1557, 2019.

[2] H. Wang, N. Zhang, E. S. Du, J. Yan, S. Han, and Y. Q. Liu, “A comprehensive review for wind, solar, and electrical load forecasting methods”, *Global Energy Interconnection*, vol. 5, no. 01, pp. 9-30, 2022.

[3] R. Yin, D. X. Li, Y. F. Wang, and W. D. Chen, “Forecasting method of monthly wind power generation based on climate model and long short-term memory neural network”, *Global Energy Interconnection*, vol. 3, no. 06, pp. 571- 576, 2020.

[4] Z. Li, L. Ye, Y. N. Zhao, X. R. Song, J. Z. Teng, and J. X. Jin, “Short-term wind power prediction based on extreme learning machine with error correction”, *Protection and Control of Modern Power Systems*, vol. 1, no. 1, pp. 9-16, 2016.

[5] Y. Cheng, T. Yi, J. F. Dai, C. G. Wang, and S. J. Wu, “Uncertainty modeling of wind power frequency regulation potential considering distributed characteristics of forecast errors”, *Protection and Control of Modern Power Systems*, vol. 6, no. 1, pp. 1-13, 2021.

[6] G. G. Chen, P. Qiu, X. R. Hu, F. J. Long, and H. Y. Long, “Research of Short-Term Wind Speed Forecasting Based on the Hybrid Model of Optimized Quadratic Decomposition and Improved Monarch Butterfly”, *Engineering Letters*, vol. 30, no. 1, pp. 73-90, 2022.

[7] G. G. Chen, B. R. Tang, Z. Z. Zhang, X. J. Zeng, and S. Y. Li, “Short-Term Wind Speed Forecasting Based on Singular Spectrum Analysis, Fuzzy C-Means Clustering and Improved SSABP”, *Engineering Letters*, vol. 29, no. 2, pp. 351-364, 2021.

[8] G. G. Chen, M. Y. Zhu, J. Huang, Y. Fu, X. C. Xie, and H. Y. Dong, “Short-term Wind Speed Prediction with Master-slave Performance Based on CNN-LSTM and Improved POABP”, *Engineering Letters*, vol. 31, no. 2, pp. 848-861, 2023.

[9] M. A. Mitchell, J. A. P. Lopes, J. N. Fidalgo, and J. D. McCalley, “Using a neural network to predict the dynamic frequency response of a power system to an under-frequency loadshedding scenario”, *Proceedings of 2000 IEEE Power Engineering Society Summer Meeting. Seattle, WA, USA*, pp. 346- 351, 2000.

[10] P. E. Utgoff, N. C. Berkman, and J. A. Clouse, “Decision Tree Induction Based on Efficient Tree Restructuring”, *Machine Learning*, vol. 29, no. 1, pp. 5-44, 1997.

[11] Q. B. Bo, X. R. Wang, and K. T. Liu, “Minimum frequency prediction based on v-SVR for post-disturbance power system”, *Electric Power Automation Equipment*, vol. 35, no. 7, pp. 83-88, 2015.

[12] R. Zhu, X. Y. Ren, Q. Yao, R. C. Tang, and H, F, Zhang, “Alloy yield prediction based on BP neural network”, *Computer Programming Skills and Maintenance*, no. 4, pp. 7-9, 2020.

[13] T. G. Li, Y. Chen, W. Zheng, Z. Q. Ma, J. P. Song, and Y. Mao, “Prediction Model of Alloy Yield Based on BP Neural Network”, *Shanxi Metallurgy*, vol. 42, no. 3, pp. 15-16, 2019.

[14] X. L. Ai, Y. S. Wang, and W. M. Tang, “Prediction of blown oxygen quantity in converter steelmaking based on BP neural network”, *Steelmaking*, vol. 29, no. 2, pp. 34-37, 2013.

[15] Y. Zhang, Y. Zhang, and T. Wu, “Estimation of state of health based on charging characteristics and back-propagation neural networks with improved atom search optimization algorithm”, *Global Energy Interconnection*, vol. 6, no. 02, pp. 228- 237, 2023.

[16] X.L. Liu, and Z. B. Li, “Influence mechanism of running sportswear fatigue based on BP neural network”, *EURASIP Journal on Advances in Signal Processing*, no. 1, pp. 61, 2021.

[17] W. Liu, F. F. Xue, Y. S. Gao, W. M. E. Tuerxun, J. Sun, Y. Hu, et al, “Wind-speed forecasting model based on DBN-Elman combined with

improved PSO-HHT", *Global Energy Interconnection*, vol. 6, no. 05, pp. 530-541, 2023.
[18] J. B. Fang, C. Zhang, and C. P. Liu, "Research on short-term wind speed prediction of wind farm based on deep learning //Jilin Electrical Engineering Society", *Proceedings of the 2022 Annual Conference of Jilin Electrical Engineering Society*. *Jilin University Press*, pp. 274-283, 2022.
[19] H.Y. Long, Y. S. He, H. Cui, Q. H. Li, H. Tan, and B. R. Tan, "Research on short-term wind speed prediction based on deep learning model in multi-fan scenario of distributed generation", *Energy Reports*, vol. 8, pp. 14183-14199, 2022.
[20] F. Shi, and X. Y. Liu, "Research on wind field prediction based on hybrid convolutional neural network algorithm", *Computational Technology and Automation*, vol. 42, no. 01, pp. 129-133, 2023.
[21] X. F. Wang, and Y. Q. Zhu, "Traffic flow prediction based on GA-BP neural network model", *Journal of Mudanjiang University*, vol. 28, no. 06, pp. 105-108, 2019.
[22] W. Sun, B. Tan, and Q. Q. Wang, "Multi-step wind speed forecasting based on secondary decomposition algorithm and optimized back propagation neural network", *Applied Soft Computing Journal*, vol. 113, pp. 107894, 2021.
[23] J. Liu, F. H. Li, and X. X. Liu, "Optimization of GA-BP neural network model and foundation pit deformation prediction", *Tunnel Construction (in English and Chinese)*, vol. 41, no. 10, pp. 1-7, 2021.
[24] Z. N. Wang, H. Jiang, and X. Q. Peng, "Improved GA-BP neural network wireless channel prediction method", *Data Acquisition and Processing*, vol. 37, no. 06, pp. 1268-1279, 2022.
[25] Z. Sun, X. N. Li, H. T. Zhang, M. A. Ikbal, and A. R. Farooqi, "A GA-BP neural network for nonlinear time-series forecasting and its application in cigarette sales forecast", *Nonlinear Engineering*, vol. 11, no. 1, pp. 223-231, 2022.
[26] G. Y. Jin, W. Feng, and Q. P. Meng, "Prediction of Waterway Cargo Transportation Volume to Support Maritime Transportation Systems Based on GA-BP Neural Network Optimization", *Sustainability*, vol. 14, no. 21, pp. 13872-13872, 2022.
[27] S. Z. Shen, X. B. Tu, J. S. Lei, K. Zhou, and J. X. Liu, "Open-air bench blasting design based on GA - BP model parameter prediction", *China Metallurgical Construction Research Institute co., LTD. Industrial Construction, 2022 Academic Conference Proceedings (ZhongCe)*, pp. 272-276 + 271, 2022.
[28] H. Bian, J. Liu, X. Liu, and D. Wang, "Research on Single point Measurement of average Wind Speed in Roadway based on GA-BP neural Network", *China Work Safety Science and Technology*, vol. 19, no. 05, pp. 57-64, 2023.
[29] P. Zhang, Y. L. Wang, L. K. Liang, X. Li, and Q. Duan, "Short-Term Wind Power Prediction Using GA-BP Neural Network Based on DBSCAN Algorithm Outlier Identification", *Processes*, vol. 8, no. 2, pp. 157, 2020.